Resonance Raman Study of Model Compounds of the Phytochrome Chromophore. 2.[1] Biliverdin Dimethyl Ester

L. Margulies*[†,‡] and M. Toporowicz[‡]

Contribution from the Seagram Centre for Soil and Water Sciences, Faculty of Agriculture, Hebrew University, Rehovot, Israel, and the Isotopes Department, Weizmann Institute of Science, Rehovot, Israel. *Received February 6, 1984*

Abstract: The analysis of the resonance Raman (RR) spectra of biliverdin dimethyl ester (BVDE) in solution was carried out using the theoretical method developed by Warshel. The RR spectra of two dipyrromethenones representing the two halves of the BVDE molecule were calculated also. BVDE appears to be in the syn-syn-syn conformation in neutral solutions. Under mildly acidic conditions a proton is likely to bind to the nitrogen atom of ring C, whereas at lower pH a second proton is introduced in the lactam group of ring A.

Bile pigments are porphyrin-related systems released by the liver after metabolic decomposition of haem in animals. During this process, haem is released from its linkage with globin and finally excreted as esterified bilirubin. However, the physiological importance of bile pigments is not only related to animal metabolism. They are also structurally related to the chromophoric system of pigments of utmost importance in the vegetal world. Typical examples are phycocyanine and phycoerythrine, involved in energy-storage and -transfer processes in blue-green algae,[2] and phytochrome (P), the pigment responsible for plant growth regulation.[3]

Although a great amount of physiological research has been done on phytochrome, most of its biochemical features remain unclear. It is known to exist in at least two different forms which differ in their physiological activity and spectroscopic characteristics. One of them (P_r) absorbs in the near-red region of the spectrum and is physiologically inactive, whereas the other form (P_{fr}) absorbs more to the far-red and is physiologically active. These two forms are interconvertible by light but only P_{fr} is able to revert in the dark and at room temperature to P_r.

Efforts have been directed to clarify the sequence of events involved in the interconverison of P, paying special attention to the chromophore, regarding its chemical, photochemical, and spectroscopic behavior.[4] An important contribution to the elucidation of the phytochrome question has been the investigation of phytochrome chromopeptides[5] which suggests a diastereomerization step in the sequence of the interconversion. This suggestion is supported by studies on model compounds for the chromophore.[4b,c,d] These investigations afforded important knowledge about the process, remaining still unclear whether a chemical reaction, a protonation equilibrium, a diastereomerization, a conformational change, or a combination of these processes lead to the striking characteristics of P.

One of the bile pigments that has been considered as a model compound for the chromophore of P is biliverdin dimethyl ester (BVDE, I). This compound has been extensively studied by using different spectroscopic techniques, such as absorption, fluorescence, circular dichroism, and ^{1}H NMR.[4c,6,7] Due to the lack of fine structure in the absorption and emission bands of this pigment, the structural information obtained by these two methods is relatively poor. However, by comparing the electronic absorption spectra with theoretical calculations of the PPP and force field types it has been possible to derive the helical conformation for this compound.[8] On the other hand, ^{1}H NMR spectroscopy was proven to be very valuable in determining the configuration of the molecule (*Z*,*Z*,*Z*) and the tautomeric situation of rings A and D (both in the lactam form).[4c] Among the spectroscopic techniques that provide detailed information about molecular structure, resonance Raman (RR) is one of the most suitable. The first measurements of RR spectra of bile pigments were reported by us in 1979[1] showing that this technique can indeed be applied to the study of these large conjugated molecules.

In this paper we report the analysis of the RR spectra of BVDE in neutral and acidic solutions using the theoretical treatment of the RR process developed by Warshel.[9] This approach is based on the calculation of the Franck–Condon factors and the differentiation of the electronic transition moments with respect to the vibrational modes. The mathematical formalism is transcribed in the Appendix.

Results and Discussion

We have used the theoretical approach described in the Appendix for calculating the RR spectrum of BVDE. Up to now this method has not been used for complex heteroatomic systems with many intramolecular degrees of freedom, like the bile pigments. Therefore, appropriate parameters for these molecules were not available. The required parameterization was carried out using the crystal coordinates of BVDE as initial data.[10] The parameters used for the σ-part were those proposed by Warshel. Different sets of parameters for the π-part have been used, ranging from those proposed by Warshel[11] to those used by Falk and

[†] Hebrew University.
[‡] Weizmann Institute of Science.

(1) Part I: Margulies, L.; Stockburger, M. *J. Am. Chem. Soc.* **1979**, *101*, 743-744.
(2) (a) Chapman, D. J. "The Biology of Blue-Green Algae"; Carr, H. G. Whitten, B. A., Eds., Blackwell: Oxford, London, Edinburgh, 1973; Chapter 3. (b) Grabowski, J.; Gantt, E. *Photochem. Photobiol.* **1978**, *28*, 39-45.
(3) (a) Kendrick, R. E. "Chemistry and Biochemistry of Plant Pigments"; Goodwin, T. W., Ed.; Academic Press: New York, 1976; Vol. 2, Chapter 23. (b) Kendrick, E.; Spruit, C. J. P. *Photochem. Photobiol.* **1977**, *26*, 201-214. (c) Pratt, L. M., *Photochem. Photobiol.* **1978**, *27*, 82-105.
(4) (a) Braslawsky, S. E.; Holzwarth, A. R.; Langer, E.; Lehner, H.; Matthews, J. I.; Schaffner, K. *Isr. J. Chem.* **1980**, *20*, 196-202. (b) Falk, H.; Grubmayr, K. *Angew. Chem.* **1977**, *89*, 487-488. (c) Falk, H.; Grubmayr, K.; Haslinger, E.; Schlederer, T.; Thirring, K. *Monatsh. Chem.* **1978**, *109*, 1451-1473. (d) Falk, H.; Grubmayr, K.; Kapl, G.; Mueller, N.; Zrunek, U. *Monatsh. Chem.* **1983**, *114*, 753. (e) Grombein, S.; Ruediger, W.; Zimmermann, H. *Hoppe-Seyler's Z. Physiol. Chem.* **1975**, *356*, 1709-1714. (f) Kuffer, W.; Cmiel, E.; Thuemmler, F.; Ruediger, W.; Schneider, S.; Scheer, H. *Photochem. Photobiol.* **1982**, *36*, 603-607. (g) Scheer, H. *Angew. Chem., Int. Ed. Engl.* **1981**, *20*, 241-261. (h) Song, P. S.; Chae, Q.; Gardner, J. *Biophys. Biochim. Acta* **1979**, *576*, 479-495.
(5) Thuemmler, F.; Ruediger, W. *Tetrahedron* **1983**, *39*, 1943-1981.
(6) Falk, H.; Haslinger, E.; Schlederer, T. *Monatsh. Chem.* **1979**, *110*, 1287-1294.
(7) (a) Blauer, G.; Wagniere, G. *J. Am. Chem. Soc.* **1975**, *97*, 1949-1954. (b) Chae, Q.; Song, P. S. *J. Am. Chem. Soc.* **1975**, *97*, 4176-4179. (c) Braslawsky, S. E.; Holzwarth, A. R.; Lehner, H.; Schaffner, K. *Helv. Chim. Acta* **1978**, *61*, 2219-2222. (d) Tegmo-Larsson, I.; Braslawsky, S. E.; Culshaw, S.; Ellul, R. M.; Nicolau, C.; Schaffner, K. *J. Am. Chem. Soc.* **1981**, *103*, 7152-7158. (e) Holzwarth, A.; Lehner, H.; Braslawsky, S.; Schaffner, K. *Liebigs Ann. Chem.* **1978**, 2002-2017.
(8) (a) Falk, H.; Hoellbacher, G. *Monatsh. Chem.* **1978**, *109*, 1429-1449. (b) Falk, H.; Mueller, N. *Tetrahedron* **1983**, *39*, 1875-1885.
(9) (a) Warshel, A.; Dauber, P. *J. Chem. Phys.* **1976**, *66*, 5477-5488. (b) Warshel A. *Annu. Rev. Biophys. Bioeng.* **1977**, *6*, 273-300.
(10) Sheldrick, W. S. *J. Chem. Soc., Perkin Trans. 2* **1976**, 1457-1462.
(11) Warshel, A., personal communication.

0002-7863/84/1506-7331$01.50/0

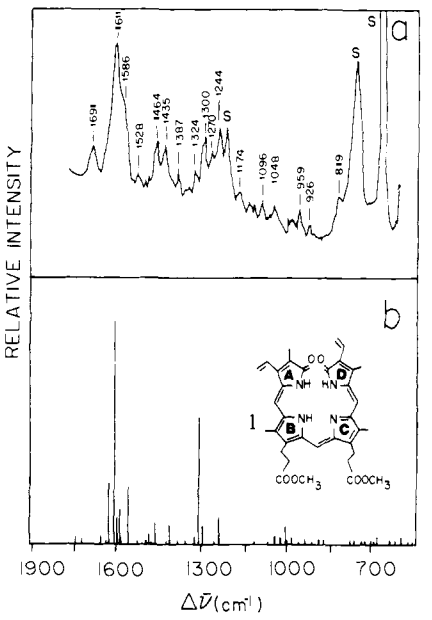

Figure 1. Experimental (a) and calculated (b) RR spectra of BVDE. The experimental spectrum was recorded exciting with λ = 5145 Å. Solvent ($CHCl_3$) lines are indicated by the letter S.

Hoellbacher[8a] in their calculations on bile pigments. It turns out that for zero π-functions the parameters suggested by Falk are those that give the best fit with experimental results, whereas, for the geometry-dependent parameters, those suggested by Warshel are the most appropriate. The resulting set of parameters used in these calculations is given in Table I. The calculated electronic transitions of BVDE are given in Table II. Figure 1 shows the RR spectrum of this molecule, evaluated at resonance with the first electronic transition together with the spectrum measured in a chloroform solution.

Using the same set of potential parameters, we have studied the method's sensitivity to changes in the molecular conformation. The calculated RR spectra of four different conformers of BVDE, obtained by 180° rotations around the single bonds of the three methene bridges, are shown in Figure 2. A strong dependence of the calculated spectra on the assumed molecular conformation was observed, proving the applicability of the theoretical method to the conformational analysis of bile pigments. Among the four conformers studied, syn-syn-syn seems to give the best fit with the experimental RR spectrum.[12] Moreover, calculations show that this is the lowest energy conformation (Figure 3). C=O stretching of the lactam groups around 1700 cm^{-1} are calculated with significant intensity only for this conformer. The syn-syn-anti conformer does not reproduce the strong band observed experimentally at 1300 cm^{-1}. The calculated RR spectrum of the anti-syn-syn conformer shows a strong band at 1675 cm^{-1}, which does not have a counterpart in the experimental spectrum. Calculations on the syn-anti-syn conformer do not reproduce the relatively strong band observed at 1435 cm^{-1}, and in addition, its calculated electronic absorption spectrum gives a wrong relationship for the intensities of the red and blue bands (Table II).

For all species studied in this work the Raman spectra were calculated in resonance with all relevant electronic transitions. The assignment of the frequency to the corresponding vibrational normal mode was made observing the variation of the normal coordinate vector due to the transition.

In order to elucidate the assignment of the RR lines, we have investigated two model compounds, that represent each half of the BVDE molecule. The calculated RR spectra of the two dipyrromethenones II and III are presented in Figure 4. They

(12) Here it is assumed that a single conformation is responsible for the measured RR spectrum. The fit between experimental and calculated spectra could probably be improved by considering the existence of more than one conformational species in solution, as indicated by the fluorescence results.[7e]

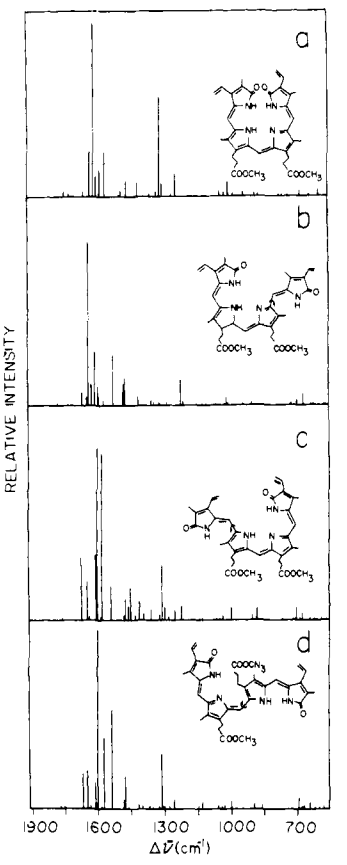

Figure 2. Calculated RR spectrum of four different conformers of BVDE. (a) SSS, (b) SSA, (c) ASS, (d) SAS.

seem to be complementary in reproducing the RR spectrum of BVDE (Table III). Bands corresponding to C=O stretching appear theoretically at 1774 cm^{-1} in II and at 1773 cm^{-1} in III which are identified with their analogues in BVDE at 1743 and 1721 cm^{-1}, respectively. In BVDE, C=C stretching in bridge A–B appears at 1623 cm^{-1} and in bridge C–D at 1606 cm^{-1}. They correspond to lines at 1682 cm^{-1} in II and 1624 cm^{-1} in III, respectively. In both cases, C=O and C=C stretching, a comparison of the spectra shows that the order of appearance in the frequency range is kept, but the vibronic transitions for the "halves" lie at higher energy. In the dipyrromethenones the conjugation is less extended; the double bonds are more localized and therefore stronger. Bands corresponding to C–C stretching in ring B of BVDE (1525 and 1460 cm^{-1}) appear only in II (1534 and 1475 cm^{-1}) while the analogous vibrations for ring C (1556 and 1408 cm^{-1}) appear only in III (1590 and 1405 cm^{-1}). C–H rocking in bridge C–D of BVDE (1308 and 1237 cm^{-1}) appears only in III (1313 and 1247 cm^{-1}). In this region, II does not present any significant lines. The strong band that is calculated at 1656 cm^{-1} for III is assigned to the exocyclic double bond located at the site where the BVDE molecule was "cut".

Protonation of BVDE

In part 1[1] we have shown that drastic changes in the frequencies and relative intensities of the RR bands of BVDE are observed in the experimental spectra when passing from a neutral solution to acidic media (compare the spectra shown in Figures 1a, 5a, and 6a). In mildly acidic solutions, among other changes, the disappearance of vibrational lines at 1244, 1300, and 1435 cm^{-1}, the appearance of a strong band at 1317 cm^{-1}, and the shift and intensity changes observed around 1600 and 1700 cm^{-1} are remarkable.

In strong acidic media new vibrational lines appear at 1267 and 1325 cm^{-1}, two strong lines of about the same intensity are observed at 1618 and 1630 cm^{-1}, and the vibration around 1700 cm^{-1} disappears. These data suggest the existence of different species depending upon the acidity of the medium.

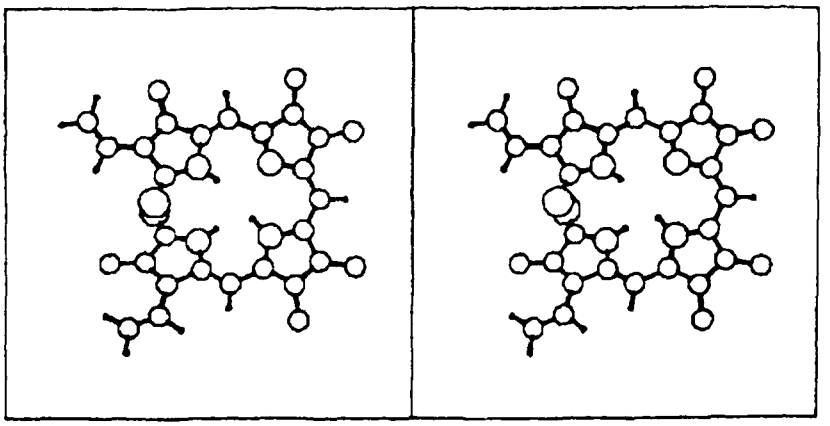

Figure 3. Stereoscopic view of BVDE in its equilibrium conformation.

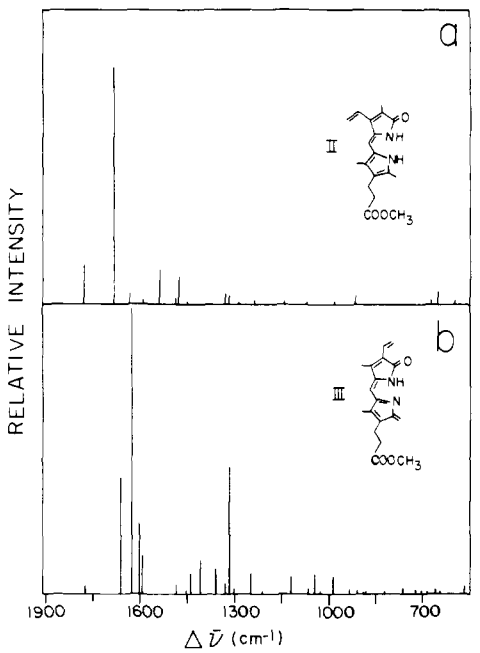

Figure 4. Calculated RR spectra of dipyrromethenones II (a) and III (b).

Single Protonation. We assume that under mildly acidic conditions, a singly protonated species of BVDE is present (cation I). The calculations on this compound were carried out testing three different possibilities of addition of a proton to three different electronegative centers in the molecule (IV, V, and VI in Figure 5). In these cases, the monocentric core integral parameter W°_{2p} for the atom that carries the proton was reduced by 15 units and its π-electronic density raised by 1. The results show that the proton is likely to bind the electronegative nitrogen atom of ring C (Figure 5b, structure IV). As discussed below, the calculated RR spectrum for this system is in better agreement with experimental results than the other two single-protonation possibilities. Here the best fit is obtained when considering resonance with the second electronic transition. It is explainable in view of the observed red shift of the red absorption band with the acidity of the medium.

The assignment of the calculated RR transitions in this species (IV) is presented in Table III. Two bands, (1817 and 1827 cm^{-1}), corresponding to C=O stretching in the lactam groups of rings A and D, respectively, appear shifted to higher energy with respect to neutral BVDE (1743 and 1721 cm^{-1}). It reproduces the effect experimentally seen: in neutral BVDE these bands are observed around 1690 cm^{-1}, but in weak acidic media they appear around 1700 cm^{-1}. For neutral BVDE there appears experimentally a band at 1435 cm^{-1} which is not observed in mildly acidic solutions. Calculations give a band at 1408 cm^{-1} for neutral BVDE, but for singly protonated species it is not found. This band is assigned

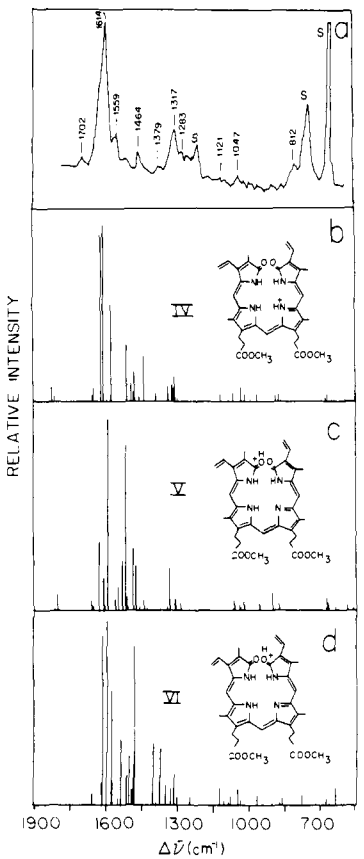

Figure 5. Experimental (a) and calculated (b, c, d) RR spectra of BVDE in mildly acidic solutions. The experimental spectrum was recorded by exciting with λ = 5145 Å. Solvent ($CHCl_3$) lines are indicated by the letter S.

to C–C stretching in ring C. The band broadening observed around 1300 cm^{-1} is well reproduced theoretically and corresponds to several bands: 1341, 1328 (N–H rocking in ring A), 1322 (C–H rocking in bridge B–C), and 1313 cm^{-1} (C–H rocking in vinyl substituent in ring A). For neutral BVDE a band is observed at 1244 cm^{-1}, which disappears under mildly acidic conditions. It is calculated at 1237 cm^{-1} for neutral BVDE but is absent in singly protonated species. This band corresponds to C–H rocking in bridge C–D. Structure V (Figure 5c) is ruled out because the theoretical calculations give a strong band at 1529 cm^{-1}, which does not match with experiment. As well, structure VI (Figure 5d) is ruled out because calculations do not show any band for the C=O stretching and three calculated strong bands are in disagreement with experiment (1482, 1404, and 1375 cm^{-1}).

Double Protonation. We assume that in strong acidic media a doubly protonated species of BVDE is present (cation II). Two possibilities have been considered for the introduction of a second

Table I. Parameters for the Potential Functions[a]

	bond function				bond function		
atoms	D_b	b	a	atoms	D_b	b	a
CH	286.4	1.0	104.0	MH	339.0	1.0	103.1
AH	339.0	1.8	103.1	MA	65.0	1.6	2.0
CC	110.3	1.9	86.0	BC	110.3	1.7	86.0
AA	87.9	1.7	1.8	BA	250.0	1.5	88.0
AC	250.0	1.5	88.0	AQ	250.0	1.5	88.0
AN	65.0	1.6	2.1	QB	110.3	1.65	86.0
AO	110.0	1.2	1.8	QH	414.0	1.0	93.0
NH	414.0	1.0	93.0				

	bond angle function						bond angle function				
atoms	K_θ	θ_o	F	K_χ	q_o	atoms	K_θ	θ_o	F	K_χ	q_o
HCH	39.5	1.911	1.7	0.0	1.80	BCA	15.5	1.911	55.0	0.01	2.45
CCH	25.3	1.911	48.9	0.0	2.20	AAN	52.8	2.094	32.0	0.0	2.564
HAH	29.4	2.094	3.0	0.01	1.90	NAO	52.8	2.094	32.0	0.0	2.564
AAH	24.0	2.094	29.5	0.0	2.178	AAO	52.8	2.094	32.0	0.0	2.564
CAH	24.0	2.094	29.5	0.0	2.178	ANA	52.8	2.094	32.0	0.0	2.564
AAC	52.8	2.094	32.0	0.0	2.564	AQB	15.5	1.911	55.0	0.01	2.45
AAA	52.8	2.094	32.0	0.0	2.564	AQH	24.0	2.094	29.5	0.0	2.178
ANH	24.0	2.094	29.5	0.0	2.178	OAQ	22.0	2.094	30.0	0.01	2.60
ACH	24.0	2.094	29.5	0.0	2.178						

	torsion function				torsion function		
atoms	$K_\phi^{(1)}$	$K_\phi^{(2)}$	$K_{\theta\theta'}$	atoms	$K_\phi^{(1)}$	$K_\phi^{(2)}$	$K_{\theta\theta'}$
-CC-	-2.3	1.161	-9.5	-AC-	0.0	-0.9	0.0
-AA-	-6.0	2.54	2.3	-AH	0.0	0.8	0.0
-AN-	-6.0	2.54	2.3	-NH	0.0	4.0	0.0

	nonbond function				nonbond function		
atoms	A	μ	B	atoms	A	μ	B
HH	19.50	1462.6	3.76	AN	718.49	89937.0	4.30
CH	120.45	11297.2	3.67	AO	573.14	39580.8	4.30
CC	746.78	92431.0	3.60	NO	562.47	339404.5	4.30
AH	120.45	11297.2	3.67	OH	79.28	12786.1	4.30
NH	117.78	41578.9	4.30	BQ	746.77	92431.0	3.60
OH	79.28	12786.1	4.20	AQ	746.77	92431.0	3.60
AA	746.77	92431.0	3.60	CQ	746.77	92431.0	3.60
NN	725.73	24911.0	4.30	QN	718.49	1189937.0	4.31
OO	393.62	108268.6	4.24	QH	120.50	11297.2	3.67

	monocentric core integrals				monocentric core integrals		
atom	$I - A$	W_{2p}^0	β'	atom	$I - A$	W_{2p}^0	β'
A	9.7	-10.0	0.2	N	16.0	-25.5	0.1
O	17.45	-17.3	0.2	M	16.0	-11.5	0.1

	bicentric core integrals						bicentric core integrals				
atoms	β_o	b_o^1	μ_β	K_β	E_1P_{ab}	atoms	β_o	b_o^1	μ_β	K_β	E_1P_{ab}
AA	-2.4	1.379	2.0356	0.4054	-0.03	AN	-1.65	1.397	1.9541	0.1039	-0.20
AO	-3.1	1.230	2.7	1.9	0.00	AM	-2.4	1.397	1.7825	0.8884	-0.20

	repulsion integrals				repulsion integrals		
atoms	G_s	G'	μ_r	atoms	G_s	G'	μ_r
AA	0.69	4.6	0.232	AN	0.3	2.75	0.451
AO	0.6	6.6	0.430	AM	0.6	-2.0	0.070

[a] A, carbon atom of sp^2 type; M, nitrogen atom of sp^2 type; B, methyl group; Q, –O– oxygen atom.

proton in the molecule (Figure 6). Changes in the parameters similar to those made in singly protonated species were made. As in singly protonated species, calculations of the RR spectrum at resonances with the second electronic transition give the best fit.

Although each of the two theoretically predicted spectra shown in Figure 6b,c could be considered for analyzing the experimental data, it seems to us that protonation on the lactam oxygen of ring A (VII) simulates somehow better the measured spectrum. For structure VIII a medium-intensity band, which is assigned to the C=O stretching in ring A, is predicted at 1739 cm^{-1}. On the other hand, for structure VII this vibration is calculated at 1504 cm^{-1}. Due to sharing of electrons with the bounded proton, a weaker C=O bond could explain this low-energy vibration.

The fact that the experimental spectrum does not present any band in the region around 1700 cm^{-1} (Figure 6a) suggests that the second protonation takes place on the lactam group of ring A. From an electrostatic point of view, this center appears to be more plausible because it is located farther from the protonated nitrogen atom of ring C than its counterpart of ring D (Table II). A band is observed at 1267 cm^{-1} in the experimental spectrum which is not observed in neutral species. It is reproduced theoretically for doubly protonated BVDE at 1272 cm^{-1} which is assigned to the O–H rocking of protonated lactam of ring A. This band is characteristic of this compound. The fact that no band is observed in this region for BVDE in mildly acidic solutions together with the disappearance of the band at 1435 cm^{-1} for both singly and doubly protonated species and which corresponds to C–C stretching in ring C supports the suggestion of the existence of doubly protonated BVDE as in structure VII.

Conclusions

In general, there is a good agreement between experimental and theoretically calculated spectra. Regarding conformational analysis the theoretical method is shown to be sensitive to geo-

Table II. Electronic Transitions of Biliverdin Dimethyl Ester

neutral									
		calcd[a]							
exptl		SSS		ASS		SSA		SAS	
ν, cm^{-1}	$\epsilon \times 10^{-3}$	ν, cm^{-1}	f	ν, cm^{-1}	f	ν, cm^{-1}	f	ν, cm^{-1}	f
15151	13[b]	18818	0.14	19901	0.39	19467	0.22	20019	0.81
		22442	0.17	22456	0.49	23234	0.70	22907	0.88
26385	45[b]	26886	0.68	26552	1.49	25404	0.80	25117	0.26

cation I				cation II			
exptl		calcd[c]		exptl		calcd[d]	
ν, cm^{-1}	$\epsilon \times 10^{-3}$	ν, cm^{-1}	f	ν, cm^{-1}	$\epsilon \times 10^{-3}$	ν, cm^{-1}	f
14837	36[e]	17269	0.58	14706	28[e]	17880	0.50
26178	52[e]	27931	0.30	26455	47[e]	27097	0.34
		28987	1.10			29863	1.30

[a] SSS, Syn-syn-syn conformation; ASS, anti-syn-syn conformation; SSA, syn-syn-anti conformation; SAS, sym-anti-syn conformation. [b] Pertier, C.; Dupuy, C.; Jardon, P.; Gautrou, R. *Photochem. Photobiol.* **1979**, *29*, 390. [c] Structure IV for cation I. [d] Structure VII for cation II. [e] Estimated from previous work part I, Ref 1).

Table III. Theoretical Assignment of Vibrational Modes (Frequencies in cm^{-1})

	BVDE	II	III	Cation I	Cation II
	1743w	1774m		1817w	1504m
	1721w		1773w	1827w	
	1623m	1682s		1625s	1629s
	1606s		1624s		
	1596m	1586w			
	1585m		1599m	1613s	1590m
	1580w			1577s	1557m
	1556m		1590w	1580w	

	BVDE	II	III	Cation I	Cation II
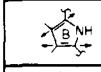	1525w	1534m		1525m	
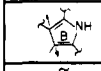	1460m	1475m		1443m	1449m
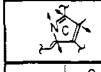	1408m		1405m		
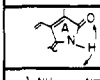				1341w 1328w	
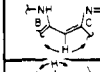				1322w	1320m
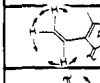				1313m	
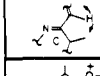	1308s 1237m		1313s 1247w	1300w	1300w
					1272m

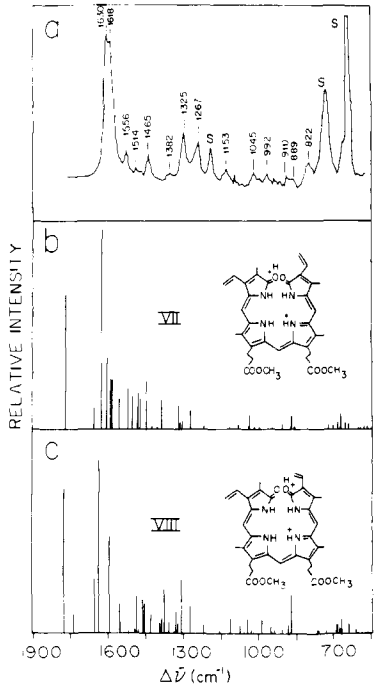

Figure 6. Experimental (a) and calculated (b, c) RR spectra of BVDE in strong acidic solutions. The experimental spectrum was recorded by exciting with λ = 5145 Å. Solvent ($CHCl_3$) lines are indicated by the letter S.

metrical alterations making it suitable for testing structural details. Moreover, protonation effects are well reproduced, revealing information that could hardly be obtained using other techniques. The discrepancy between calculated and observed relative intensities of some bands (e.g., C–H rocking in bridge C–D of BVDE at 1308 cm^{-1} and C=O stretching in the propionic chain of doubly protonated BVDE) are due to the inherent approximations of the method. A further refinement of the method or an exhaustive revision of the potential parameters could improve the accuracy of the calculations. Nevertheless the main characteristics of the studied systems are well described, demonstrating the power of the method in assessing structural features in complex molecules.

Acknowledgment. We are indebted to Professors A. Warshel, A. Yogev, and H. Falk for helpful discussions and to R. Sharon and P. Dauber for able computer assistance.

Appendix: Warshel's Method for Calculation of RR Spectra

In order to calculate the ground and excited potential surfaces the usual σ–π separation is made, setting the σ-part as an empirical potential function of the CFF form[13] and calculating the π-part in the frame of the PPP-SCF method, corrected for nearest-neighbor orbital overlap. The general expression for the potential function is

$$V^M(r) = V_\sigma(r) + V_\pi^\circ(r) + \Delta V_\pi^M(r)$$

where $V_\sigma(r) + V_\pi^\circ(r)$ is the sum of the σ- and π-electron energies for the ground state and $\Delta V_\pi(r)$ is the π-electron excitation energy.

(13) Lifson, S.; Warshel, A. *J. Chem. Phys.* **1968**, *49*, 5116.

$V^M(r)$ is taken as function of the coordinates to permit a fast evaluation of it and of its first and second derivatives. $V_\sigma(r)$ includes contributions from bonding, bond angle, torsion angle, and nonbond interaction terms and is introduced as an analytical function of the coordinates,

$$V_\sigma(r) = \tfrac{1}{2}\sum_i D_b[\exp(-2a(b-b_o)) - 2\exp(-a(b-b_o))] + \tfrac{1}{2}\sum_i K_\theta(\theta_i-\theta_o)^2 + \tfrac{1}{2}\sum_i K_x(x_i-x_o)^2 + \tfrac{1}{2}\sum_i F(q_i-q_o)^2 + \tfrac{1}{2}\sum_i K_\phi^{(1)}\cos\phi_i + \tfrac{1}{2}\sum_i K_\phi^{(2)}\cos 2\phi_i + \tfrac{1}{2}\sum_i K_{\theta\theta'}(\theta_i-\theta_o)(\theta'_i-\theta_o)\cos\phi_i + \sum_{ij}[A\exp(-\mu r_{ij}) - Br_{ij}^{-6}]$$

where b_i are bond distances, θ_i are bond angles, ϕ_i are torsion angles, q_i are 1-3 nonbonded distances, r_{ij} are all higher order nonbond distances, and x are out of plane angles. D, a, b, K_θ, θ_o, F, q, K_x, K_ϕ, $K_{\phi'}$, $K_{\theta\theta'}$, A, B, and μ are adjustable parameters which depend on the type of atoms involved.

The π-potential term, corrected for nearest-neighbor orbital overlap is

$$V_\pi^\circ(r) = \sum_\mu P_{\mu\mu}(r)[{}^\lambda W_\mu(r)P_{\mu\mu}(r){}^\lambda\gamma_{\mu\mu}(r) + \tfrac{1}{4}P_{\mu\mu}(r){}^\lambda\gamma_{\mu\mu}(r)] + 2\sum_{\mu<\nu} P_{\mu\nu}(r){}^\lambda\beta_{\mu\nu}(r) - \sum_{\mu<\nu}[\tfrac{1}{2}P_{\mu\nu}{}^2(r) - Q_\mu(r)Q_\nu(r){}^\lambda\gamma_{\mu\nu}]$$

where $P_{\mu\mu}$ is the π-electron density on the μth atom, $P_{\mu\nu}$ is the π-bond order between atoms μ and ν, ${}^\lambda W_\mu$ and ${}^\lambda\beta_{\mu\nu}$ are the core integrals, ${}^\lambda\gamma_{\mu\mu}$ is the Coulomb integral for the μth atom, and ${}^\lambda\gamma_{\mu\nu}$ is the interchange integral for atoms μ and ν, all corrected for nearest-neighbor orbital overlap. Q_μ are the atomic charges.

$V_\pi^\circ(r)$ is set in analytical form in terms of zero order π-functions and its dependence on the geometry of the system, to introduce the appropriate adjustable parameters:

$${}^\lambda W_\mu = W_{2p}^\circ + \beta'[\exp(-2\mu_\beta(b_{\mu,\mu+1} - b_o{}^1))\cos^2 t_{\mu,\mu+1}]$$

$${}^\lambda\beta_{\mu,\mu\pm1} = \beta_o\exp(-\mu_\beta(b_{\mu,\mu\pm1} - b_o{}^1))(1 + K_\beta(b_{\mu,\mu\pm1} - b_o{}^1))\cos(t_{\mu,\mu\pm1})(1 - E_tP_{\mu,\mu\pm1}\cos(t_{\mu,\mu\pm1}))/(1 - E_tP_{\mu,\mu\pm1})$$

$${}^\lambda\gamma_{\mu,\mu} = (I - A) + G_s[\exp(-2\mu_\beta(b_{\mu,\mu\pm1} - b_o{}^1))\cos^2(t_{\mu,\mu\pm1})]$$

$${}^\lambda\gamma_{\mu,\nu} = G'\exp(-\mu_\gamma r_{\mu,\nu}) + e^2/(D + r_{\mu,\nu})$$

where $t = {}^1/_2(\phi_1 + \phi_2 + \phi_3 + \phi_4)$, with ϕ_i the torsional dihedral angles of the conjugated bond and $r_{\mu,\nu}$ the distance between atoms μ and ν.

The excitation energy $\Delta V_\pi{}^M$ is given by

$$\Delta V_\pi{}^M(r) = \sum_\nu R_\nu{}^{W\lambda}W_\nu(r) + \sum_\nu R_{\nu\nu}{}^\gamma{}^\lambda\gamma_{\nu\nu}(r) + \sum_{\nu<\mu} R_{\mu\nu}{}^\beta{}^\lambda\beta_{\mu\nu}(r) + \sum_{\nu<\mu} R_{\mu\nu}{}^\gamma{}^\lambda\gamma_{\mu\nu}(r)$$

with $R_\nu{}^W$, $R_{\nu\nu}{}^\gamma$, $R_{\mu\nu}{}^\beta$, and $R_{\mu\nu}{}^\gamma$ excitation coefficients.

With this expression for $V^M(r)$, the equilibrium geometry is found and the mass scaled Cartesian origin shift

$$\Delta^M = M^{-1/2}(r_{eq}{}^M - r_{eq}{}^G)$$

with M a diagonal matrix of the atomic masses, is evaluated. The complete set of vibrational frequencies ν and the normal coordinates vectors $\mathbf{L}$ can be evaluated by diagonalizing the matrix of mass scaled Cartesian second derivatives of $V^M(r)$ at the calculated minimum. In this way it is possible to identify each Raman frequency with its normal vibrational mode. The relative intensities are proportional to the Franck-Condon factors.

Registry No. I, 10035-62-8; II, 92219-97-1; III, 92219-98-2; IV, 68996-06-5; VII, 88471-57-2.

Photoelectron Spectroscopy of Isomeric C_4H_7 Radicals. Implications for the Thermochemistry and Structures of the Radicals and Their Corresponding Carbonium Ions

Jocelyn C. Schultz, F. A. Houle, and J. L. Beauchamp*

Contribution No. 6699 from the Arthur Amos Noyes Laboratory of Chemical Physics, California Institute of Technology, Pasadena, California 91125. *Received December 27, 1983*

Abstract: The first photoelectron bands of 1-methylallyl, 2-methylallyl, allylcarbinyl, and cyclobutyl radicals have been obtained. Adiabatic and vertical ionization potentials respectively are 7.49 ± 0.02 and 7.67 ± 0.02 eV for the 1-methylallyl radical, 7.90 ± 0.02 and 7.95 ± 0.02 eV for the 2-methylallyl radical, 8.04 (+0.03, −0.1) and 8.47 ± 0.05 eV for the allylcarbinyl radical, and 7.54 ± 0.02 and 7.66 ± 0.02 eV for the cyclobutyl radical. With use of known or estimated radical heats of formation, heats of formation of the corresponding carbonium ions are calculated to be 203.1 ± 1.4 kcal/mol for the 1-methylallyl cation, 212.2 ± 1.6 kcal/mol for the 2-methylallyl cation, 231.0 ± 3 kcal/mol for the allylcarbinyl cation, and 225.1 ± 1.1 kcal/mol for the cyclobutyl cation. Vibrational progressions of 990 ± 100 and 410 ± 30 cm^{-1} are resolved on the first photoelectron bands of the cyclobutyl radical and the 2-methylallyl radical, respectively. Vibrational structure is observed on the 1-methylallyl radical photoelectron band, but vibrational progressions could not be assigned. The complex spectrum probably results mainly from the fact that it is ascribed to two isomers, *cis*- and *trans*-1-methylallyl radicals. The presence of vibrational structure on the first photoelectron bands of these radicals is consistent with the ions being at local minima on the $C_4H_7^+$ potential surface. Major thermal decomposition and isomerization products of 1-methylallyl, 2-methylallyl, allylcarbinyl, cyclobutyl, and cyclopropylcarbinyl radicals are identified in the photoelectron spectra. No thermolysis products of the 2-methylallyl radical are observed. A small amount of 1,3-butadiene and/or 2-butene is observed at high temperatures from the 1-methylallyl radical. Pyrolysis of the allylcarbinyl radical yields the 1-methylallyl radical and 1,3-butadiene. Due to its facile ring opening to the allylcarbinyl radical (which is observed along with its thermolysis products), the cyclopropylcarbinyl radical itself is not observed. Pyrolysis of the cyclobutyl radical yields 1-methylallyl and 1,3-butadiene. The allylcarbinyl radical, the direct product of the cyclobutyl radical ring opening, is not observed, presumably because it is formed with sufficiently high internal energy to further rearrange rapidly.

In solution, numerous experiments have been performed to gather structural, spectroscopic, and kinetic data on $C_4H_7^+$ under stable ion and solvolytic conditions in order to characterize the intermediate(s) involved in the cyclopropylcarbinyl, cyclobutyl,

0002-7863/84/1506-7336$01.50/0